Kinetics of the Condensation Reaction of Epoxide with Phenol: Linear Chain Growth versus Branching

Mark E. Smith and Hatsuo Ishida*

NSF Center for Molecular and Microstructure of Composites, Department of Macromolecular Science, Case Western Reserve University, Cleveland, Ohio 44106

ABSTRACT: The melt state reaction of the diglycidyl ether of Bisphenol A with Bisphenol A is investigated with respect to modeling the reaction rate. Both linear chain addition and branching are considered within the general model as well as the probability for unreactive site formation in the branching reaction path. Through the use of Fourier transform infrared spectroscopy, the epoxide concentration is monitored using the 913-cm^{-1} band. The phenol mode at 1592 cm^{-1} provides the necessary second parameter as an internal thickness band for the application of the nonlinear regression technique. Two modifications of a general model are evaluated for the A + B → C and A + C → C type reaction systems. The results of the regression analysis are in close agreement under different considerations of unreactive site probability. Catalysis effects upon the branching reaction are found to be negligible for model accuracy for the stoichiometric samples. The activation energy calculated from the rate constants determined is in excellent agreement with those reported in the literature.

Introduction

Epoxies are employed in a near-endless variety of applications, from bulk structural composite matrices to thin specialty coatings. Most interest in the study of these materials has historically been focused upon the resulting materials—that is to say, the properties that are exhibited by the product regardless of the underlying molecular direction and influence upon these properties. Typical discussion on epoxy resins relates primarily to the type of curing agent, curing cycle, and/or cured properties.

The melt state reaction of Bisphenol A with the diglycidyl ether of Bisphenol A (DGEBA) is a simple procedure for producing higher molecular weight oligomers of the DGEBA structure. However, fundamental information on this route of polymerization remains largely unreported in the literature to date. Of the few studies available, the majority consider the solution reaction of this material, neglecting the complications that arise in the absence of solvent. With regard to the melt, the effects of the phenolic species[1] and the behavior of conversion with respect to type of alcohol have been reported.[2] There has also been valuable work performed on the role of catalyst on the extent of branching in more recent years.[3,4] While the mechanisms of copolymerization of cyclic anhydrides with epoxy resin have been definitively studied in both solution[5] and the melt,[6] practical knowledge of the phenol–epoxy reaction kinetics and effects on final material properties remains insufficient.

Figure 1 presents a schematic representation of the copolymerization reaction. Linear addition proceeds as shown by k_1 to produce an alcohol group pendant to the chain backbone. Subsequent to the formation of this species, the terminal epoxide group can react with this pendant hydroxyl group to form a branch, depicted as k_2. Continued branching reactions will ultimately produce a cross-linked material.

In this paper, kinetic analysis is performed by the application of Fourier transform infrared spectroscopy (FT-IR). With this technique, direct measurement of functional species present within a sample can be performed as a function of reaction time. In-situ experiments can readily be undertaken through the use of temperature-controlled sample holders mounted within the spectrometer. The approach of using the FT-IR technique for kinetic investigations has been well documented for many materials, including epoxy systems.[6-10]

Experimental Section

The diglycidyl ether of Bisphenol A, Epon 825, and Bisphenol A, polycarbonate grade, were obtained from Shell Chemical Corp. The catalyst, *p*-(chlorophenyl)-1,1-dimethylurea, was manufactured by DuPont. All materials were stored over desiccant and used as received without further purification.

A monofunctional epoxide was synthesized for model compound studies. Epichlorohydrin and cumylphenol (Aldrich) were reacted in refluxing methyl ethyl ketone with sodium hydroxide (2 wt %). The cumylphenol was added dropwise to minimize reaction of the produced monoepoxide compound with the cumylphenol. The solution was neutralized with HCl and then washed twice with aqueous NaOH solution to remove unreacted cumylphenol. Purification was performed by separation on a silica gel column utilizing hexane/ethyl acetate (80/20%) solvent. Identification and purity of the compound were determined by FT-IR, ^{1}H-NMR, and reverse-phase high-performance liquid chromatography (HPLC), utilizing a C-18 Novapak column (Waters Chromatography). The sample was determined to be of a purity level in excess of 99%.

A Bomem Michelson MB single-beam Fourier transform infrared spectrometer was employed for the experimental data collection. This spectrometer is equipped with a liquid-nitrogen-cooled mercury–cadmium–telluride (MCT) detector for data collection in the region 5000–500 cm^{-1} and a dry nitrogen gas purge. The specific detectivity, D^*, of the MCT detector is 1.0 × 10^{10} cm Hz$^{1/2}$/W. Spectra were collected using the autosequencing mode of the spectrometer with fixed time delays. Spectra were collected as 5 coadded interferograms every 5.5 s for the 160 and 150 °C reactions and as 5 coadded interferograms every 30 s for 140 °C. For the lower temperatures, 5 coadded spectra were collected with an 80-s time interval. The model compound reactions were performed at 120, 140, and 160 °C and were monitored as 2 coadded spectra at time intervals which allowed a minimum of 15 spectra to be collected prior to 50% conversion of the monoepoxide. All spectra were obtained by the acquisition of raw spectra which were later referenced to a paired set of raw spectra collected without sample. This procedure allowed the effects of atmospheric water and emissive contributions from the temperature employed to be minimized. The sample chamber was purged with dry nitrogen at the rate of 120 cm^3/s during each kinetic experiment.
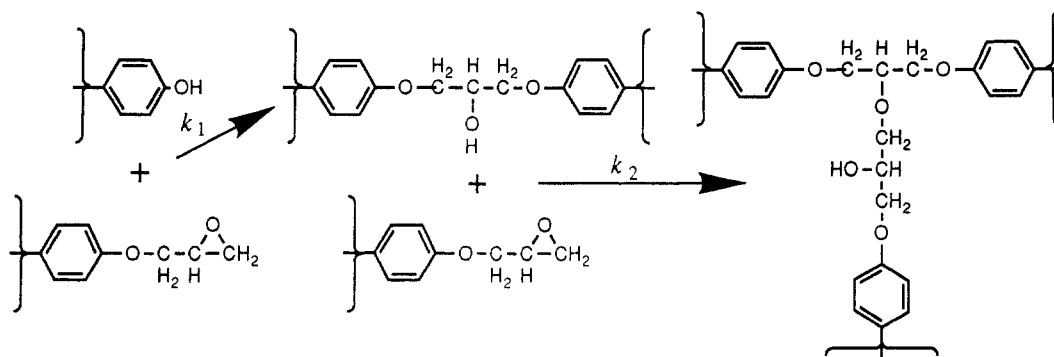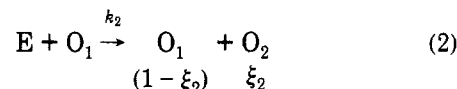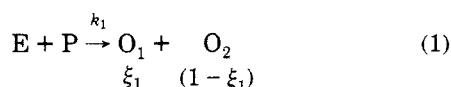
Figure 1. Schematic representation of the reaction of Bisphenol A and the diglycidyl ether of Bisphenol A. Linear addition denoted by k_1; branch formation depicted as k_2.

Samples were prepared by dissolving the epoxide and the phenol with p-(chlorophenyl)-1,1-dimethylurea into two spectrophotometric grade acetone solutions. The concentration of catalyst, when present, was maintained at the level of 2% of the total weight of the reactants. These solutions were prepared in stoichiometric proportions at low concentrations, ~ 0.003 M (1.0000 g of diepoxide in 10 mL of acetone). Equal volumes of the two solutions were pipetted and mixed immediately before the experiments. For the DGEBA/Bisphenol A studies, the solvent mixed reactants were then cast by syringe as 0.1 mL of solution onto a KBr plate which was preheated and thermally equilibrated in a transmission-geometry heated cell sample holder. The cell was rapidly placed in the beam path, and data collection was initiated upon closing the sample chamber of the instrument. The solvent evaporation rate was sufficiently rapid that no contribution to the initial spectrum was discernible. The model compound reaction procedure was analogous except for the sampling geometry. These experiments employed a temperature-controlled attenuated total reflection (ATR) attachment from Harrick Scientific. This attachment was modified in our laboratory for kinetic studies of fast-reacting, low-viscosity systems[7] and was equipped with a single-reflection zinc selenide prism for this study. The low molecular weight of the model compounds necessitated the use of the horizontal substrate to prevent the sample from flowing out of the optical path of the infrared beam. The temperature of the heated samples was monitored and controlled with a proportional–integral–derivative (PID) temperature controller equipped with a type J thermocouple located adjacent to the sample substrate, and the sample was maintained at ±1 °C. During the initial measurements, it was found that the low viscosity of the materials did allow some flow and/or leveling of the solution-cast material as evidenced by a decrease in the aromatic absorbance until a stable film of material was achieved in the beam path.

Spectral analysis was performed with in-house software programs written in Fortran 77 and run on a Digital MicroVax II computer. For the kinetic analysis the concentration versus time data were functionalized to remove random noise and allow interpolation when necessary. Each concentration versus time curve was fit to a second-order polynomial such that the correlation coefficient was at least 0.99. The rate constants for the kinetic models were computed using software incorporating a nonlinear statistical method, Systat Version 5.2 (SYSTAT Inc.), operating on a Macintosh computer. In addition to linear least-squares analysis, this program allowed the analysis to be performed by both a quasi-Newton[13] and a Simplex[14] method. Both methods were employed as a measure of the final parameter accuracy. The aromatic stretching absorbance bands at 1510 and 1607 cm^{-1} were used as internal standard bands.

Approach

The reaction of the diglycidyl ether of Bisphenol A (E), with Bisphenol A (P) can be expressed most generally as

$$E + P \overset{k_1}{\rightarrow} \underset{\xi_1}{O_1} + \underset{(1-\xi_1)}{O_2} \qquad (1)$$

$$E + O_1 \overset{k_2}{\rightarrow} \underset{(1-\xi_2)}{O_1} + \underset{\xi_2}{O_2} \qquad (2)$$

where k_1 and k_2 are the rate constants for each reaction and ξ_1 and ξ_2 are the fractional components of species O, where O_2 is unreactive with the diepoxide. This condition is included to allow for the possibility of both primary and secondary alcohols forming upon opening of the oxirane ring. From these expressions, the rate of change of each component can be expressed in general terms as

$$-d[E]/dt = k_1[E][P]^n + k_2[O_1][E][P]^{n-1} \qquad (3)$$

$$-d[P]/dt = k_1[E][P]^n \qquad (4)$$

$$d[O_1]/dt = k_1\xi_1[E][P]^n + k_2\xi_2[O_1][E][P]^{n-1} \qquad (5)$$

where $n = 1$ or 2, allowing for a catalytic effect of the Bisphenol A on the reaction rates. When eq 5 is divided by eq 4 and integrated with the boundary condition that initially $P = 1.0$ and $O_1 = 0.0$, we obtain

$$\frac{O_1}{P} = \frac{\xi_1[1 - P^{(\xi_1\kappa - 1)}]}{\xi_1\kappa - 1} \qquad (6)$$

where $\kappa = k_2\xi_2/k_1\xi_1$. Equation 3 can be rearranged to

$$-\frac{d \ln E}{dt} = k_1 P^n \left[1 + \frac{\xi_1 k_2 (1 - (P/P_0)^{(\xi_1\kappa - 1)})}{k_1(\xi_1\kappa - 1)} \right] \qquad (7)$$

Similarly, eq 3 and 4 can be combined to yield

$$(E_0 - E) = (P_0 - P)\left(1 + \frac{\xi_1 k_2}{k_1(\xi_1\kappa - 1)}\right) - \frac{\xi_1 P_0}{\xi_2}\left(\frac{1 - (P/P_0)^{\xi_1\kappa}}{\xi_1\kappa - 1}\right) \qquad (8)$$

where the zero subscript indicates the initial concentration of the reacting species. Thus, eqs 7 and 8 provide the relationship necessary to determine the terms containing the parameters k_1, k_2, ξ_1, and ξ_2 using data for both epoxide and phenol concentration as a function of reaction time.

It has been found that this resin system demonstrates gelation phenomena in the range of 60–75% conversion of epoxide.[14] Since this condition imposes mobility restrictions upon the chains, the kinetics will certainly be affected beyond this conversion level. The inability of the functional groups to freely encounter each other should be expected to reduce the rate of consumption of phenolic species and possibly cause an apparent enhancement in
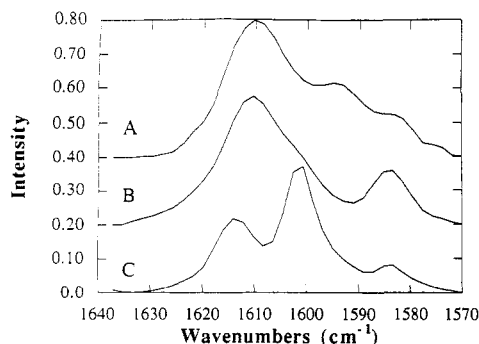
Figure 2. FT-IR absorbance spectra of (A) DGEBA/Bisphenol A mixture, (B) glycidyl ether of cumylphenol, and (C) cumylphenol.

the pendant alcohol–epoxide reaction. Our interest in the competing reactions lies prior to gelation; thus, the analysis of the kinetic parameters will be focused upon the reaction prior to 60% epoxide conversion to eliminate any diffusion limitation effects on the parameters.

Results and Discussion

Epoxide concentration can be directly determined using the characteristic epoxide absorbance band at 913 cm^{-1}. The hydroxyl groups cannot be as readily monitored. Considerable hydrogen-bonding effects make the intensity variation unreliable for concentration determination in the OH stretching region (3700–3100 cm^{-1}). In consideration of the ether stretching region (1140–1085 cm^{-1}), contributions from the oxirane ring ($\sim$1266 cm^{-1}, weak), the [CH$_2$–O–Ar] linkage ($\sim$1248 cm^{-1}, strong), and the phenolic species ($\sim$1225 cm^{-1}, strong) are heavily overlapped and, as such, frustrate simple analysis. While curve-resolving techniques could be applied to separate the overlapped bands, the hydrogen bonding also leads to band shape changes which are no longer strictly Lorentzian.[9]

In consideration of the reaction itself, the phenol is consumed by the loss of a hydrogen atom in the process of substitution on the CH$_2$ terminal group of the oxirane. The aromatic stretching region near 1600 cm^{-1} represents "quadrant stretching" of the ring carbon atoms.[11,12] Different groups located *para* on the ring give rise to not only a loss of symmetry but also a dipole moment change which in turn influences the infrared vibrations. These bands can be strong when one group is a *meta* director, O–R, and the other is an *ortho–para* director, alkyl as is the case in our product.

As shown in the previous section, kinetic analysis requires that the concentrations of both epoxide and phenol species be determinable throughout the reaction. The epoxide is readily measured by its absorbance at 913 cm^{-1}. By use of the model compounds, cumylphenol and the glycidyl ether of cumylphenol, insight into the nature of the quadrant stretching of the aromatic rings of these compounds is obtained. Figure 2 presents the infrared spectra for this frequency region of the DGEBA/Bisphenol A mixture (A), the glycidyl ether of cumylphenol (B), and cumylphenol (C). The large absorbance at 1610 cm^{-1} is clearly visible in both the resin mixture and the monoepoxide. In addition, the absorbance band at 1582 cm^{-1} is discernible in all three of the compounds. Table 1 lists the assignments of these bands with respect to the compounds studied. The strong band at 1600 cm^{-1} is strikingly evident in the cumylphenol sample and does contribute weakly to the monoepoxide spectrum as determined by spectral curve resolving. From these

Table 1. Infrared Absorbance Band Assignments for Kinetic Analysis of Phenol Concentration

	1610 cm^{-1}	1600 cm^{-1}	1592 cm^{-1}	1582 cm^{-1}
DGEBA/ Bisphenol A	strong	very weak	medium	weak
DGEBA	strong	very weak	very weak	medium
Bisphenol A	strong	very weak	medium	very weak
cumylphenol	medium	strong	very weak	weak
monoepoxide	strong	weak	very weak	medium
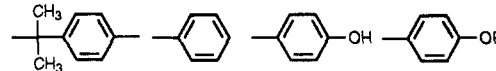
findings, the band at 1592 cm^{-1} can be assigned to the Bisphenol A structure within the mixed resin samples. The 1610-cm^{-1} band becomes an internal reference band for normalization of the concentration within the beam path. Comparison of the intensity of the 1610-cm^{-1} band with that of the 1510-cm^{-1} band, another widely used internal thickness band for benzene derivatives, showed an excellent agreement.

The spectral changes which occur during the reaction of DGEBA with Bisphenol A are illustrated in Figure 3 for the reaction temperature of 130 °C. The absorbance in the aromatic stretching region has been resolved into the three structural contributions: 1610, 1592, and 1582 cm^{-1}. From this figure, one can see that the Bisphenol A component becomes nearly indiscernible without the aid of curve resolving after 20 min of reaction time. The concentration of the Bisphenol A decreases to 40% of its initial value. Considering the epoxide absorbance, the strong band in the initial spectrum also decreases greatly to a level of 10% of the original value. While not entirely obvious from the four spectral regions shown, there is a large imbalance between the amount of epoxide consumed as compared to Bisphenol A.

To better demonstrate this imbalance in monomer consumption, Figure 4 presents the concentration of epoxide and phenol species as a function of reaction time. In addition, this figure contains the same information for a sample deficient in Bisphenol A [r = 0.66 ((moles of Bisphenol A)/(mole of DGEBA))] and a sample which contained no catalyst.

Comparing the observed behavior for these samples with respect to epoxide consumption we note two key features. First, it is apparent that the initial rate of epoxide consumption in each case is nearly identical when the stoichiometric ratio is equal to 1.0 irrespective of the presence of catalyst. The sample without catalyst begins to decrease in rate of both epoxide and phenol consumption when the level of phenol species decreases below 60% of the initial value. This result suggests that phenol species that are acting as catalyst become less effective when gelation is approached. The second observation on epoxide consumption is that the extent of reaction is decreased either when Bisphenol A is deficient or when no external catalyst is present. This finding is not unusual since the continued consumption of epoxide would be with the secondary hydroxyl groups. As reported by Doszlop et al.,[16] the solution reaction of phenol and epoxide was found to proceed to a level of 50% at which point the phenolic species activated the branching reaction. Since the material is known to be past gelation at this stage,[15,17] the mobility of phenol species to assist in further reaction is severely limited.

The phenolic consumption of Figure 4 also lends insights into the reaction. For r = 0.66, the initial rate of consumption is analogous to that of the r = 1.0 sample and that of the sample without catalyst, as indicated for
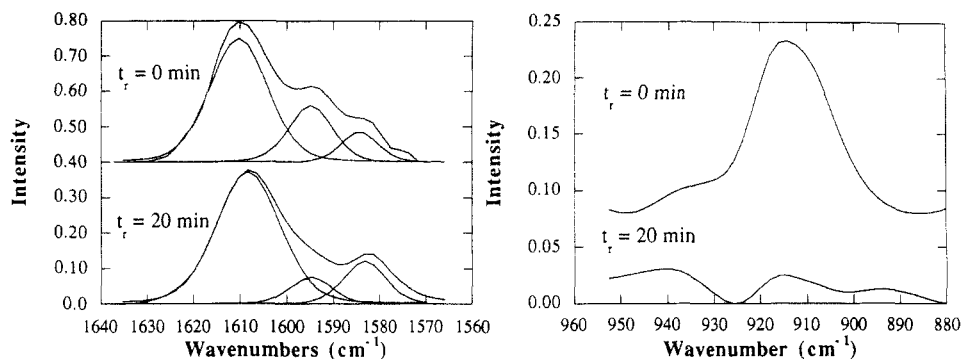
Figure 3. FT-IR absorbance spectra of DGEBA/Bisphenol A reaction at reaction times of 0.0 and 20 min in the 1640–1560 and 960–880-cm^{-1} regions. Isothermal reaction at 130 °C.
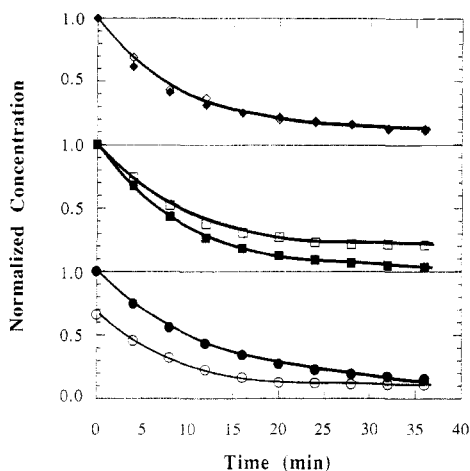

Figure 4. Epoxide and phenol concentration profiles as a function of reaction time (T = 130 °C) for three compositions: (O) stoichiometric ratio r = 0.66; (□) r = 1.0; (dvo) r = 1.0, no catalyst. Solid symbols denote epoxy concentration; open symbols denote phenol concentration.

the initial slope. The amount of unreacted Bisphenol A becomes constant regardless of initial molar concentration. As a result, the remaining Bisphenol A may serve as terminal units to the chains and branches and is unable to react with a proximate epoxide group. Most dramatic is the sample containing no catalyst. Throughout the reaction the consumption of epoxide and phenol is identical. This finding shows that there may be a suppression of the branching mechanism in the absence of external catalyst because the ring-opening reaction would be catalyzed by a phenol species as depicted below:
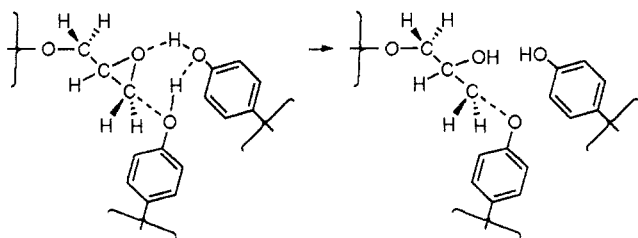
In this case the increased steric hindrance for reaction of the secondary hydroxyl would further discourage the branching reaction.

The nonstoichiometric data yield much information on the effects of Bisphenol A content when simply analyzed as above; nevertheless, the true value of these data for our investigation is in determination of the exponent n for the reaction rate dependence on phenol concentration, (eqs 3–5). Considering the rate of phenol consumption, the slope of the curves in Figure 5 shows that for r = 1.0 the
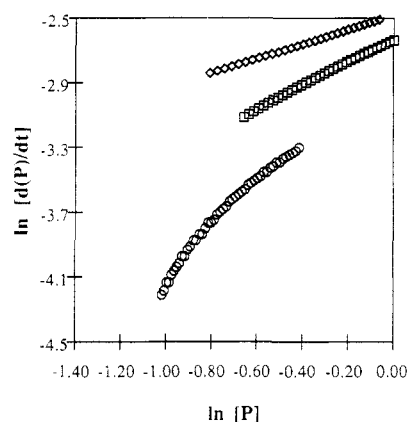

Figure 5. Plot determining the kinetic order of phenol consumption as a function of phenol concentration: (O) stoichiometric ratio r = 0.66; (□) r = 1.0; (◊) r = 1.0, no catalyst.
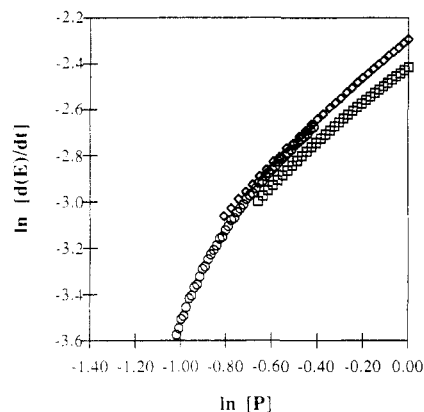

Figure 6. Plot determining the kinetic order of epoxide as a function of phenol concentration: (O) stoichiometric ratio r = 0.66; (□) r = 1.0; (◊) r = 1.0, no catalyst.

exponent has a value nearly equal to 1.0 and for r = 0.66 the initial value is identical to the equimolar sample but steadily increases with Bisphenol A consumption. In contrast, the sample without catalyst follows a value of 0.5 for the entire reaction. These results necessitate that the values of n in eq 4 equal 1.0 for the equimolar sample analysis. When we consider the epoxide consumption, Figure 6, the order is more uniform for the different mixtures. At the beginning of the reaction, all three samples show a dependence of 1.0 with respect to phenol concentration. The stoichiometric samples, with and without catalyst, behave the most linear with a slope nearly equal to 1.0. The Bisphenol A deficient sample initially follows a first-order dependence which increases as the phenol is consumed. Most importantly, we may now assume a value of n = 1.0 for eq 3 and the linear regression determination of the kinetic parameters based on the

Table 2. Rate Constants Determined by Differential Analysis where $O_1 = f(1 - P)$

temp (°C)	k_1 (min^{-1})	fk_2 (min^{-1})	R^2
110	0.038	0.056	0.9968
120	0.053	0.087	0.9990
130	0.089	0.153	0.9978
140	0.123	0.250	0.9932
150	0.308	0.679	0.9928
160	0.564	0.987	0.9940
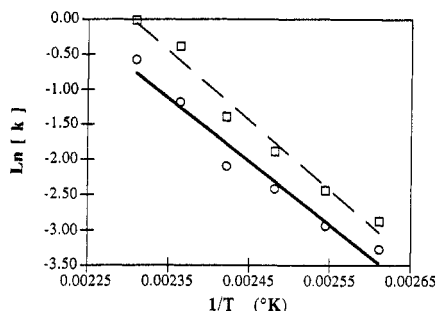
Figure 7. Arrhenius plot of the rate constants k_1 (O) and κk_2 (□) as determined by the differential form of Case 1. Activation energy determined as 17.9 ± 1 kcal/mol for linear reaction (k_1) and 19.7 ± 1 kcal/mol for branch reaction (k_2).

stoichiometric sample behavior. From both theory and the work of other researchers, the order of the reaction should be 1.0 with respect to the epoxide concentration for the linear condensation reaction.[1,18,19]

Two cases were considered in determination of the kinetic parameters in eq 7. Each case will be presented with a brief discussion.

Differential Form

Case 1:

$$O_1 = f(1 - P)$$

Under these conditions, the reaction proceeds as each phenol reacting produces a secondary alcohol, some fraction (K) of which is then used to react with an epoxide. Also, each secondary alcohol which reacts does not produce a species capable of further reaction. This second condition can be imposed due to the steric effects created at the branch site. Equation 6 then becomes

$$-\frac{d \ln E}{dt} = k_1 P + k_2 f(1 - P) \qquad (9)$$

This is the most simple case where the analysis is based on the determination of the rate constants and f only.

The results of this analysis are collected in Table 2. The averaged standard error associated with the values of k_1 and fk_2 were consistently <3%. The least squares fit of the data yields an excellent fit over the temperature range studied as evidenced in the values of R^2.

The results of this analysis are shown in Figure 7 in the determination of the activation energy for each reaction mode of the epoxide through an Arrhenius plot of the rate constants. From these data, the activation energy for the epoxide ring opening by a phenol group is determined as 17.9 ± 1 kcal/mol. At the same time, the energy for ring opening by a secondary alcohol is found to be higher at 19.7 ± 1 kcal/mol. These values are near those found previously and are well within the range typically reported in the literature for the epoxide ring opening.

Case 2:

$$\frac{O_1}{P} = \frac{\xi_1[1 - P^{(\xi_1 \kappa - 1)}]}{\xi_1 \kappa - 1}$$

Within the context of the molecular significance, this case allows some fraction ξ_1 of the secondary hydroxide species produced by the linear reaction to undergo further reaction with epoxide. In addition, for those secondary hydroxyl groups which do react, a fraction ξ_2 deactivate that hydroxyl site for further epoxide consumption. This analysis yields an equation of the form

$$-\frac{d \ln E}{dt} = k_1 P + \frac{k_2 \xi_1[1 - P^{(\xi_1 \kappa - 1)}]}{\xi_1 \kappa - 1} \qquad (10)$$

The results of this analysis are summarized in Table 3. Calculation of the activation energy yields a similar fit to the data of the more simple case discussed above (Figure 8). The activation energies are determined as 18.1 ± 1 and 18.3 ± 1 kcal/mol for k_1 and k_2, respectively. The identity of these two values lies in the exponential term contained in the equation representing the secondary hydroxyl reaction. As listed in the table, this value decreases from the value of 1.3 at 110 °C to the value of 0.5 for the temperatures of 140 °C and above. This exponent is explicitly attached to the curvature of the data and when fixed at the value of 0.5 yielded a poor fit to the experimental data for the lower temperatures. The significance of this result may be related to the molecular mobility and/or the extent of hydrogen bonding within the system. When the temperature is increased, the functional dependence on phenol concentration is decreased. Secondly, it bears reiterating that the values of k_2, ξ_1, and ξ_2 are strongly coupled. When either ξ_1 or ξ_2 increases, k_2 must decrease to compensate.

Integrated Form

Case 1: When we impose the condition $O_1 = f(1 - P)$ into eq 7, we obtain

$$(1 - E) = \left(1 - \frac{fk_2}{k_1}\right)(1 - P) - \frac{fk_2}{k_1} \ln [P] \qquad (11)$$

where the integration limits at the beginning of the reaction have been imposed ($E_0 = 1$; $P_0 = 1$). The parameter as determined by least squares fit is contained in Table 4. The ratio fk_2/k_1 is seen to be nearly constant at 0.18 except for the data at 140 °C, which dictates an identical correspondence between epoxy and phenol consumption. When this ratio is compared to the values obtained for the differential analysis of this case, Table 2, the agreement is seen to follow only for the lower temperatures. Since the values should be consistent in both tables, the model cannot correctly describe the chemical reaction.

Case 2: Upon integration of eq 10 and imposing the initial concentration boundary conditions

$$(1 - E) = \left(1 + \frac{k_2 \xi_1}{k_1(\xi_1 \kappa - 1)}\right)(1 - P) -$$

$$1 + \frac{\xi_2}{\xi_1(\xi_1 \kappa - 1)}(1 - P^{\xi_1 \kappa}) \qquad (12)$$

Parameters determined from this analysis are shown in Table 5. For this model, the values determined by the differential and integrated forms of the equation are in much better agreement. The ratios $\xi_1 k_2/k_1$ calculated using

Table 3. Rate Constants As Determined by the Differential Method: Complex O_1 Concentration Profile

temp (°C)	k_1 (min⁻¹)	$\xi_1 k_2$ (min⁻¹)	$(\xi_1 \kappa - 1)$	R^2
110	0.038	0.061	1.3	0.9983
120	0.053	0.089	1.1	0.9981
130	0.090	0.145	0.8	0.9996
140	0.125	0.225	0.5	0.9988
150	0.312	0.618	0.5	0.9979
160	0.577	0.856	0.5	0.9999
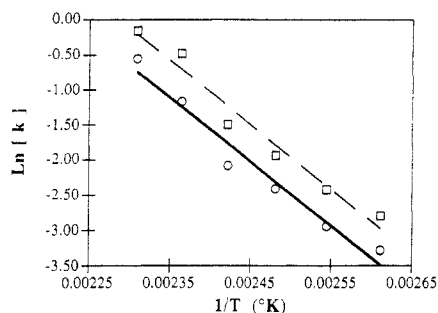
Figure 8. Arrhenius plot of the rate constants k_1 (O) and κk_2 (□) as determined by the differential form of Case 2. Activation energy determined as 18.1 ± 1 kcal/mol for linear reaction (k_1) and 18.3 ± 1 kcal/mol for branch reaction (k_2).

Table 4. Rate Constants Determined by Integral Analysis of Simple O_1 Concentration Profile

| temp (°C)	fk_2/k_1	R^2	temp (°C)	fk_2/k_1	R^2
110	0.210	0.9855	140	0.000	0.9952
120	0.176	0.9983	150	0.132	0.9994
130	0.198	0.9984	160	0.156	0.9983

Table 5. Rate Constants Determined by Integral Analysis of Complex O_1 Combination Profile

temp (°C)	$\kappa k_2/k_1$	$\xi_1 \kappa$	R^2
110	0.549	2.3	0.9873
120	0.700	2.1	0.9943
130	0.767	1.8	0.9957
140	0.000	1.5	0.9950
150	0.983	1.5	0.9961
160	1.170	1.5	0.9962

the data of Table 3 are nearly identical with those of Table 5 except for the difference of 1 introduced through the integration. The disagreement for 140 °C is again observed as a result of the overlapping concentration profiles. The variation for the 160 °C data is not obvious; however, the accuracy of the numerical fits is strongly influenced by the value of the exponent, and the ratio of 1.5 obtained from Table 3 for the ratio of rate constants is equal to the value of the exponent, which would destroy the weighting of the exponential term.

As a test of the quality of fit for the analyses performed, Figures 9 and 10 illustrate the concentration of epoxide versus the concentration of phenol for the reaction at 110 and 160 °C, respectively. The value of epoxide concentration is calculated from the integrated forms of both cases discussed (eqs 11 and 12). For the low reaction temperature the agreement of both cases is found to be within the experimental error of the data. The major distinction between the two models rests in the curvature described by the Case 2 equation. For the data of 160 °C, the models behave in the same manner.

As compared to the rate constant k_1 determined by the use of the monofunctional model compounds, the values for the DGEBA/Bisphenol A system were consistently higher. In addition, the branching reaction in the model systems was observed to affect the epoxide consumption significantly beyond 50% epoxide conversion. This finding leads to another approach in the determination of the
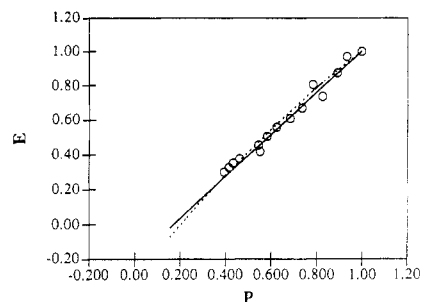
Figure 9. Comparison of concentration data with calculated data for epoxy concentration at reaction temperature 110 °C. Solid line represents Case 1 fit, dashed line represents Case 2 fit, and circles are actual data.
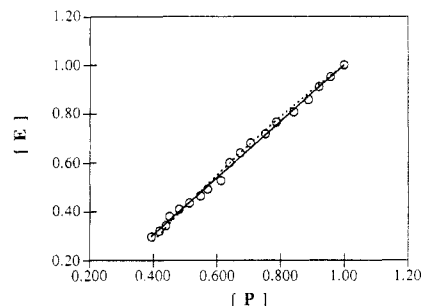
Figure 10. Comparison of concentration data with calculated data for epoxy concentration at reaction temperature 160 °C. Solid line represents Case 1 fit, dashed line represents Case 2 fit, and circles are actual data.

kinetic parameters. The underlying limitation of the general model presented is that it relies on only the phenol and epoxide concentrations as a function of reaction time. While the differential behavior does yield values, the integrated form cannot. It is important to note the significance of the disagreement in the rate constants of the model compound materials as compared to the DGEBA/Bisphenol A resin system. Not only is it possible that there is a minor molecular weight or substitution effect on the functional group reactivities, but the importance of stoichiometric ratio and the great potential for catalytic effects within this system cannot be ignored.

If we consider the reaction of epoxide and Bisphenol A as depicted in eqs 1 and 2, a fraction of the hydroxyl groups produced, ξ_1, are capable of reacting with an epoxide group. As a consequence, $(1 - \xi_1)$ groups must be unreactive due to reasons such as steric hindrance or even being an alternate structure. Similarly, we have allowed ξ_2 of the hydroxyl groups of the epoxide to become unreactive. We can now impose the restriction that $\xi_2 = (1 - \xi_1)$ if we assume that the reaction product of a phenol species and an epoxide is analogous to the product of the secondary hydroxide and epoxide. This assumption imposes an important reduction in the degrees of freedom in the model expressions.

At this point we return to the rate expressions, eqs 3-5. Our earlier analysis and discussion have shown that eq 4 correctly expresses the change in phenol concentration, where $n = 1$. In addition, we know that the first term of eq 3 must correspondingly agree. However, we may expand the second term to allow phenolic catalysis of the branching reaction. Equation 3 then becomes

$$-d[E]/dt = k_1[E][P] + k_2[O_1][E][P] \qquad (13)$$

Consequently, eq 5 becomes

$$d[O_1]/dt = k_1\xi_1[E][P] + k_2\xi_2[O_1][E][P] \qquad (14)$$

Table 6. Rate Constant Parameters Determined for Different Stoichiometric Bisphenol/Epoxide Ratios (130 °C)

BPA/DGEBA	case 1 k_2/k_1	R^2	case 2 $\xi_1(k_2/k_1)$	$\xi_1\kappa$	R^2
0.66	0.187	0.9977	0.656	1.8	0.9998
0.90	0.097	0.9998	0.276	1.8	0.9999
1.00	0.114	0.9990	0.767	1.8	0.9957
1.10	0.366	0.9726	0.795	1.8	0.9751

where the value of $n = 1.0$ has been included. Dividing eq 13 by eq 4, we obtain

$$\frac{d[E]}{d[P]} = 1 + \frac{k_2[O_1]}{k_1} \qquad (15)$$

which can be simplified by the expression for $[O_1]$:

$$\frac{d[E]}{d[P]} = 1 + \frac{k_2\xi_1}{k_1(1-\xi_1)}(1 - e^{-\{(k_2/k_1)(1-\xi_1)(1-P)\}}) \qquad (16)$$

This expression contains the condition of $\xi_2 = (1 - \xi_1)$. This equation becomes valuable when the exponential term is expanded into a series about $P = 1.0$. Then, neglecting higher order terms

$$(1 - E) = (1 - P)\left(\frac{1 + \xi_1}{1 - \xi_1}\right) \qquad (17)$$

With this expression, the values of ξ_1 can be determined from the data of Table 4. Overall, the epoxy consumption is increased as compared to phenol consumption corresponding to $\xi_1 = 0.08 \pm 0.02$.

The phenolic catalysis of the secondary hydroxyl reaction with epoxide has been previously reported by Doszlop et al.[16] Their work found that, in the absence of catalyst, the branching reaction occurs during the initial stages of reaction and that the activation energy of the secondary hydroxyl reaction with epoxide exhibited a larger activation energy as compared to that of the phenol-epoxy reaction.

The final discussion of the appropriateness of the models to the reaction relies upon the comparison of the fit to nonstoichiometric data. For stoichiometric ratios of $r = 0.66$, 0.9, 1.0, and 1.1 [(moles of Bisphenol A)/(mole of epoxy)], the reaction at 130 °C was analyzed. The parameters determined from the Case 1 and Case 2 models are listed in Table 6. Except for the values determined for $r = 0.90$, the values appear to be nearly constant with a steady increase as a function of temperature for the Case 2 model. For each temperature the epoxide is consumed faster than the phenol as observed in the stoichiometric data above.

Overall, the numerical analysis demonstrates that the consumption of epoxide and phenol follows an expected second-order reaction for the linear chain growth mode, while the branching reaction may involve a catalytic contribution from the phenol species. While the models employed for this study do not explicitly predict the concentration dependence of the two species as a function of reaction time, the molecular significance of the model outweighs the error demonstrated ($\leq 5\%$) in determining the kinetics through gelation. In addition, errors from both the regression analysis and the curve-resolving

procedure must be recognized with respect to the acceptability of the model error.

Conclusions

The two rate constants for the linear chain addition mode and the branching mode of the copolymerization of the diglycidyl ether of Bisphenol A with Bisphenol A in the melt state were determined using numerical analysis on FFIR concentration data. The activation energy of the linear mode was found to be 18 ± 1 kcal/mol while the branching mode relies upon a higher value of 20 ± 1 kcal/mol. When the model is expanded to include higher order terms in the representation of secondary alcohol concentration, the activation energies become nearly equal at 18 ± 1 kcal/mol for both the linear and branching reactions.

The aromatic stretching region, 1600–1550 cm⁻¹, contains the information on phenol species concentration with negligible hydrogen-bonding distortions which are present in the OH stretching and ether regions of the spectra. Through analysis of model compounds, a characteristic phenol absorbance has been determined to occur at 1592 cm⁻¹.

The use of both linear least squares and nonlinear regression analysis allows the determination of the kinetic parameters which describe this reaction without information on the concentration of the secondary alcohol. Without consideration of catalysis, the models were found to reasonably predict the correlation of epoxide–phenol concentration as a function of reaction time.

Allowing catalytic influence of the phenol species yields an approximation model which closely represents the experimental concentration profiles. This catalytic model can be expressed as a series to incorporate the epoxy concentration dependence on phenol to terms of increasing order. Although the model deviates slightly from the experimental behavior, the direct molecular significance of this model justifies its use for prediction of the reaction rates prior to gelation.

References and Notes

(1) Lidarik, M. *Kunstst.-Rundsch.* **1959**, *6*, 6.
(2) Alvey, F. B. *J. Appl. Polym. Sci.* **1969**, *13*, 1473.
(3) Zahir, S. A.; Bantle, S. In *Epoxy Resin Chemistry II*; ACS Symposium Series 221; Bauer, R. S., Ed.; American Chemical Society: Washington, DC, 1983.
(4) Senger, J. S.; Subramanian, R.; Ward, T. C.; McGrath, J. E. *Poly. Prepr. (Am. Chem. Soc., Div. Polym. Chem.)* **1986**, *27* (2), 144.
(5) Luston, J.; Manasek, Z.; Kulickova, M. *J. Macromol. Sci., Chem.* **1978**, *A12* (7), 995.
(6) Antoon, M. K.; Koenig, J. L. *J. Polym. Sci., Polym. Chem. Ed.* **1981**, *19*, 549.
(7) Ishida, H.; Scott, C. *J. Polym. Eng.* **1986**, *6*, 201.
(8) Adams, M. R. *Anal. Chem.* **1964**, *36*, 1688.
(9) Morgan, R. J.; Mones, E. T. *J. Appl. Polym. Sci.* **1987**, *33*, 999.
(10) Stevens, G. C. *J. Appl. Polym. Sci.* **1981**, *26*, 4279.
(11) Colthup, N. B.; Daly, L. H.; Wiberley, S. E. *Introduction to Infrared and Raman Spectroscopy*, 2nd ed.; Academic: New York, 1975.
(12) Katritzky, A. R. *Q. Rev. Chem. Soc.* **1959**, *13*, 353.
(13) Fletcher, R. *AERE-R.* **1972**, 7125.
(14) O'Neill, R. *Appl. Stat.* **1971**, 338.
(15) Ishida, H.; Smith, M. E. *Rheol. Acta* **1991**, *30*, 184.
(16) Doszlop, S.; Vargha, V.; Horkay, F. *Period. Polytech. Chem. Eng.* **1978**, *22*, 253.
(17) Ishida, H.; Smith, M. E. *Polym. Eng. Sci.* **1992**, *32* (2), 136.
(18) Smith, J. M. *Chemical Engineering Kinetics*; McGraw-Hill: New York, 1981.
(19) Wachenfeld, E.; Burchard, W. *Polymer* **1987**, *28*, 817.